Indian Journal of Pure & Applied Physics
Vol. 59, June 2021, pp. 462-467

Orange Photoluminescence from Hydrothermally Grown Zno Nanorods and Study on its Defects

K Sowri Babu[a,b], P Sanguino[b], R Schwarz[b], L Santos[c], S Alves[c], A Fedorov[c],
V Himamaheswara Rao[d], J N Kiran[a] & Ch Sujatha[e]

[a]Vignan's Foundation for Science Technology and Research (Deemed to be) University, Vadlamudi, Andhra Pradesh, India.
[b]Departamento de Física and CeFEMA, Instituto Superior Técnico, P-1049-001 Lisboa, Portugal
[c]Department of Chemical Engineering and CQE, Instituto Superior Técnico, P-1049-001 Lisboa, Portugal
[d]Department of Physics, PACE Institue of Technology and Sciences, Ongole, Andhra Pradesh, 523 272, India.
[e]Department of Physics, RGUKT Basar, Nirmal, Telangana 504107, India.

Received 22 February 2019; accepted 28 April 2021

The visible photoluminescence (PL) of ZnO is controversial for a long time. At present, the contribution of oxygen interstitial defects to yellow/orange emission from ZnO nanostructures is on debate. In this report, the origin of orange emission from solution- grown ZnO nanorods is investigated using excitation wavelength dependent photoluminescence PL, PL excitation and UV-Vis spectra. These results showed that orange emission may be due to the transition of an electron from shallow defect levels positioned slightly below the conduction band to the singly ionized oxygen vacancies. Hence, it is believed that oxygen interstitials may not be responsible for orange emission from solution grown ZnO nanostructures.

Keywords: ZnO nanorods, Photoluminescence, Defects, Semiconductor nanostructures.

1 Introduction

ZnO is one of the prominent wide and direct band gap semiconductors having potential applications in optoelectronic devices, sensors, biomedical applications, radiation detectors *etc.*[1-3]. The importance of ZnO in diverse fields is due to its wide band gap of 3.37 eV and large exciton binding energy of 60 meV. The detailed understanding of defect luminescence of ZnO nanostructures is necessary for its use in various applications such as photo detectors, light emitting diodes *etc.*[4] In spite of the extensive research on ZnO nanostructures, visible photoluminescence (PL) or defect PL of ZnO is still controversial. It is believed that, yellow/orange PL from ZnO nano structures is attributed to the oxygen interstitials for a long time[2-7]. But, recently, Jinpeng Lv *et al.* studied origin of orange emission from hydrothermally grown ZnO nanorods through oxygen plasma exposure and low temperature O_2 annealing. Their experimental results showed that isolated interstitial oxygen is not responsible for the orange emission from ZnO and they assigned it to lithium related impurities or surface ligands[2]. Biroju *et al.* reported that orange emission is due to the shallow energy levels below the conduction band to the oxygen interstitials (O_i) in ZnO nanorods grown on graphene[4]. However, they did not mention about type of defects that introduced shallow levels below conduction band. Very recently, Amin *et al.* investigated the origin of orange/red emissions from vertically aligned zinc oxide nanorods arrays produced using hydrothermal process followed by plasma treatment in argon/sulfur hexafluoride (Ar/SF6) gas mixture for different time[8]. These results indicated that orange/red emissions are due to the transitions from conduction-band minimum (CBM) to oxygen interstitials (O_i) and CBM to oxygen vacancies (V_O) with corresponding photon energies of 2.21 and 1.90 eV, respectively[8]. It is discernable that there is no consensus on the origin of these orange/red or orange/yellow emissions. Hence, understanding the origin of orange emission from ZnO nanorods needs to be addressed.

In this work, vertically aligned ZnO nanorods are grown on glass substrates. These nanorods exhibited intense orange/red emission. Excitation wavelength dependent PL and PL excitation and absorption spectra are used to understand the initial and final states of orange emission. These results showed that orange emission is due to the transition of charge carrier from a shallow donor which is slightly below the conduction band to the oxygen vacancy.

*Corresponding Author: (E-mail sowribabuk@gmail.com)

2 Experimental Details

Zinc Acetate dihydrate $Zn(CH_3CO_2)_2 \cdot 2H_2O$ (98% sigma Aldrich), Zinc nitrate hexahydrate $Zn(NO_3)_2.6H_2O$ (98%, sigma Aldrich) and Hexamethylenetetramine ($C_6H_{12}N_4$) (sigma Aldrich) were used without further purification for the preparation of ZnO seed layers and for the growth of ZnO nanorods on glass substrates.

2.1 Preparation of the samples

Vertically aligned ZnO nanorods were prepared through two step process. In the first step, seed layer was deposited on the substrates using spin coating method. Subsequently, growth of ZnO nanorods was achieved by hydrothermal process. Before the deposition of seed layer, glass substrates were cleaned with acid, acetone and isopropyl alcohol. To prepare, ZnO seed layers on glass substrates, $Zn(CH_3CO_2)_2 \cdot 2H_2O$ was dissolved in 30 ml of distilled water to obtain 10 mM concentration. This solution was coated onto the glass substrate using spin coater at a speed of 2000 rpm. This process was repeated several times to obtain the desired thickness to grow vertically aligned ZnO nanorods. In the next step, these ZnO seed layers were immersed vertically in a solution containing $Zn(NO_3)_2.6H_2O$ and Hexamethylenetetramine (($C_6H_{12}N_4$). ZnO nanorods of different aspect ratio were grown by changing the concentration of zinc nitrate and HMTA in the ratio of 25:25, 50:50, 150:150 and 250:250 mM and the growth time was kept as 90 minutes. As prepared nanorods were rinsed with distilled water many times and dried in the ambient atmosphere.

2.2 Characterization Techniques

The morphology of the samples was studied using Field emission scanning Electron Microscope (FE-SEM). Band gap of ZnO nanorods was determined from the UV-vis absorption spectrum. The emission and excitation spectra were recorded by using the photoluminescence spectrometer (Flourolog-III).

3 Results and Discussion

Figure 1 Shows the FE-SEM pictures of ZnO seed layer and nanorods prepared with different precursor concentrations on glass substrates. Figure 1 (a-b) shows the plane and cross sectional view of the ZnO seed layer. The surface of the seed layer is uniform and the size of the ZnO nano crystallites is around 10 nm. The thickness of the seed layer measured form the Fig. 1(a) is approximately 150 nm. Figure 2 shows the Energy Dispersive Spectroscopy of ZnO nanorods. The EDS spectrum exhibits the characteristic peaks of Zn and oxygen and indicates

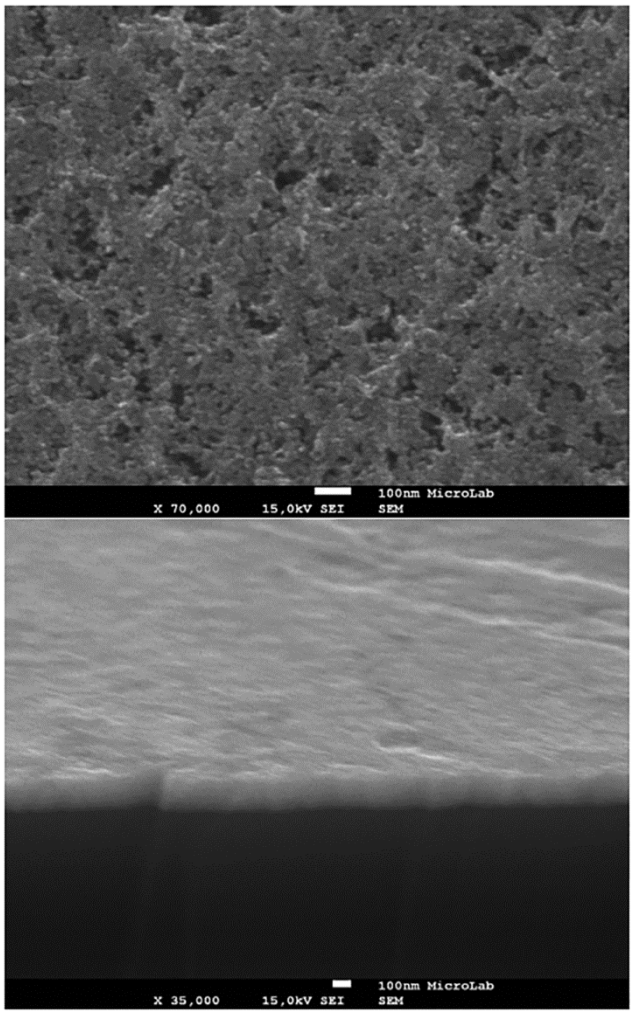

Fig. 1 — FE-SEM mages of ZnO seed layer

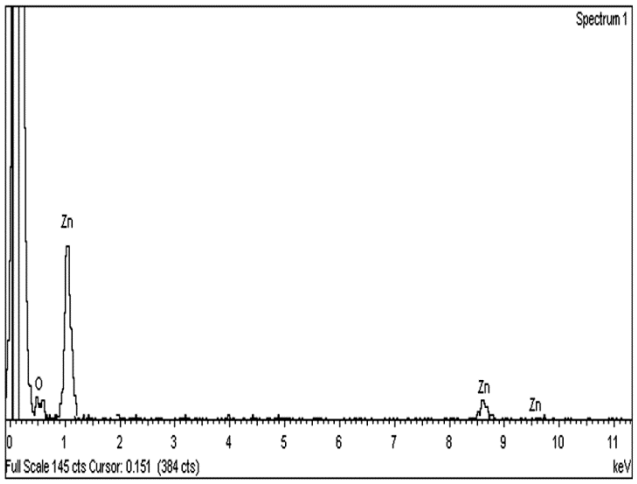

Fig. 2 — EDS spectrum of ZnO nanorods

there are no impurities in the ZnO nanorods. Figure 3(a-d) shows the cross sectional view of the ZnO nanorods grown at different concentrations of zinc nitrate and HMTA precursors (ZG1, ZG3 and ZG4). It is obvious that nanorods were grown along the c-axis (0001) with flat hexagonal tips at all concentrations. It confirms the hexagonal wurtzite structure of ZnO nanorods. However, the density and diameter of ZnO nanorods increased with increase of precursor concentration. Further, at lower concentrations (25:25 and 50:50 mM), ZnO nanorods were poorly aligned in vertical direction but at other concentrations, nanorods aligned vertically along the c-axis. The aspect ratio values for these ZnO nanorods are shown in Table 1.

Figure 4(a) shows the PL spectra of ZnO nanorods grown on glass substrates by hydrothermal method with different concentrations of precursors. Figure 4(b) shows the positions of UV emission peaks of ZnO nanorods for different concentrations. These PL spectra exhibited a very feeble near band edge (NBE) emission positioned at 377 nm and a broad and intense orange emission centered at 620 nm. The NBE emission is due to the radiative recombination of excitons and the orange emission at 620 nm was previously assigned to the interstitial oxygen ions (O_i^-)[2,4,7-8]. Since broad PL band is asymmetrical, it can be inferred that the PL band should have more than one origin. Hence the PL spectrum is Gaussian fitted to find the number of peaks in this broad PL spectrum. Figure 5 shows the PL spectrum Gaussian divided into three sub-bands (Coefficient of

Table 1 — Aspect ratio's of ZnO nanorods prepared with different precursor concentrations

Sample name	Diameter (nm)	Length (nm)	Aspect Ratio(l/d)	$P=I_{NBE}/I_{DLE}$
ZG1	55	1100	20	
ZG2	65	600	9.23	0.023
ZG3	135	650	4.81	0.035
ZG4	180	603	3.35	0.025

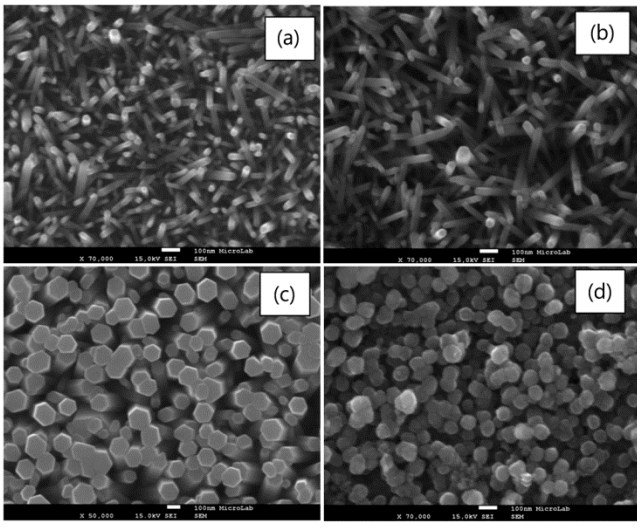

Fig. 3 — FE-SEM pictures of ZnO nanorods

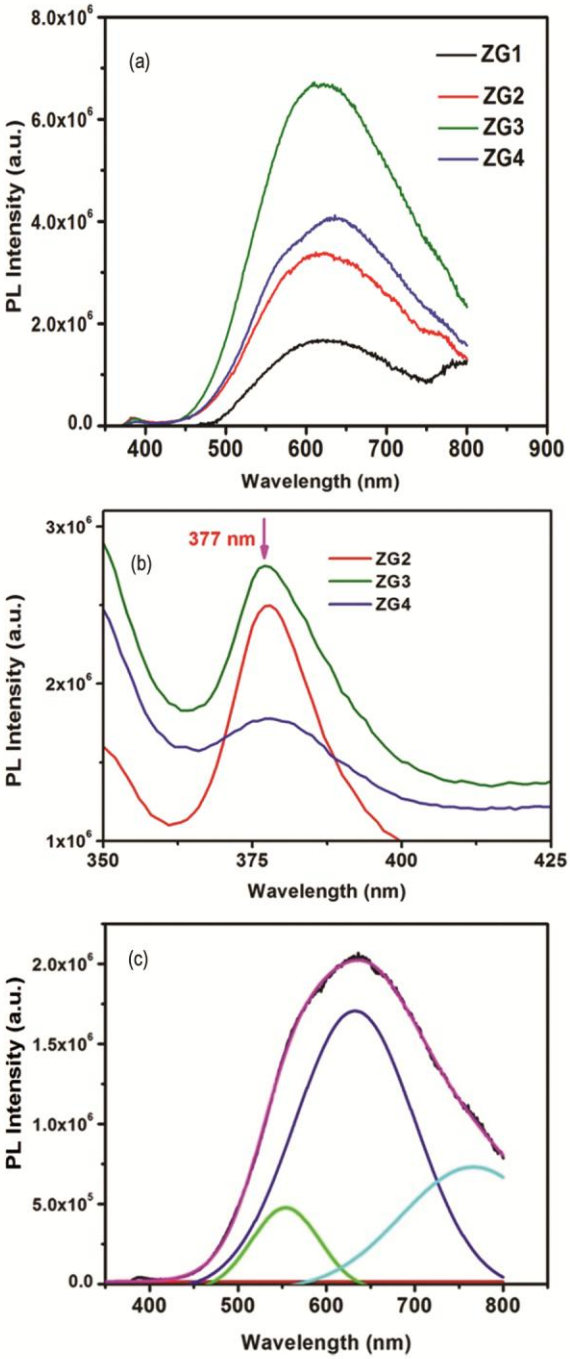

Fig. 4 — PL spectra of ZnO nanorods

determination = 0.999) positioned at 550, 620 and 754 nm respectively. The peak at 754 nm is the second order near band edge emission. The broad PL emission band containing green and orange emissions was observed by Zhang *et al*. in amorphous ZnO granular films and attributed them to oxygen vacancies and oxygen interstitials[9-10].

However, controversial mechanisms have been reported for the origin and positions of initial and terminal states responsible for these emissions. In the literature, oxygen vacancies, zinc vacancies, oxygen interstitials, zinc interstitials, Cu impurities have been assigned as a source of green emission observed in ZnO nanorods[8,11]. However, many people believed that green emission is due to singly ionized oxygen vacancies. From Fig. 4 it is obvious that ZG3 shows high intensity compared to other samples. From the FE-SEM analysis it is clear that diameter of the nanorods increased with increase of concentration and there is no considerable change in the length of the

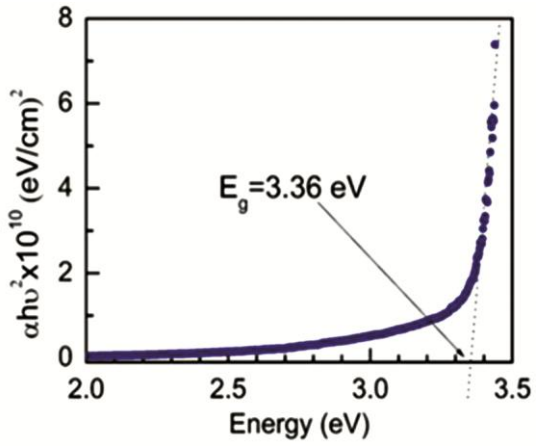

Fig. 5 — UV-v is absorption spectrum of ZnO nanorods (ZG3).

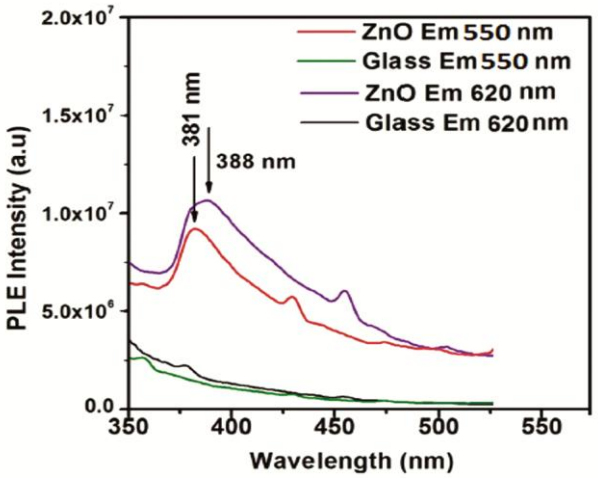

Fig. 6 — PL excitation spectra of ZnO nanorods (ZG3).

ZnO nanorods. The change in diameter is predominant when the concentration increased from 50:50 to 150:150 mM. In other words, sample having larger diameter showed highest intensity. Recent reports on PL of ZnO nanorods showed enhancement of oxygen related defects in larger diameter ZnO nanorods[12]. Hence the enhancement in the intensity of orange emission may be ascribed to the enhancement of oxygen related defects.

Since two types of defects (oxygen vacancies and oxygen interstitials) are responsible for this broad PL band[8], it can be inferred from these PL spectra that the number of oxygen vacancies and oxygen interstitials in smaller diameter nanorods happens to be same. But in larger diameter ZnO nanorods, the concentration of oxygen interstitials might have enhanced significantly compared to the oxygen vacancies. From this discussion, it is easy to understand that the broadening of PL band of larger diameter ZnO nanorods is due to the enhancement in the concentration of these defects. The initial and final states responsible for green and orange emissions are investigated by using the UV-v is absorption spectroscopy, excitation wavelength dependent PL and PL excitation spectra. Fig. 5 shows the UV-v is absorption spectrum of ZnO nanorods (ZG3). According to Tauc, for a direct semiconductor, by plotting $(\alpha h\upsilon)^2$ as a function of $h\upsilon$, the optical band gap (*Eg*) can be extracted by performing a linear fit on the linear region of high absorption according to the following equation.

$$(\alpha h\vartheta)^2 = A\,(h\vartheta - E_g) \qquad \ldots 1$$

Where $h\upsilon$ is the photon energy, α is the absorption coefficient, and A is a constant[13]. This is the equation of a straight line where the value of intercept with the abscissa axis is *Eg*. The band gap obtained is 3.36 eV which is corresponding to the wavelength of 370 nm.

Figure 6 shows the PLE spectra of glass and ZG3 acquired at different emission wavelengths. PLE of glass shows no peaks at emission wavelengths 550 and 620 nm but PLE of ZnO nanorods showed a peak at 381 nm when emission wavelength was monitored at 550 nm and broad peak centered at 388 nm when excitation wavelength was monitored at 620 nm. From the UV-v is and PLE spectra it is clear that the initial states for the green and orange emissions are lies ~0.04 and ~0.1 eV below the conduction band minimum. From Fig. 7 it is also clear that the intensity of orange emission decreased as the wavelength increased from 310 to 360 nm and then

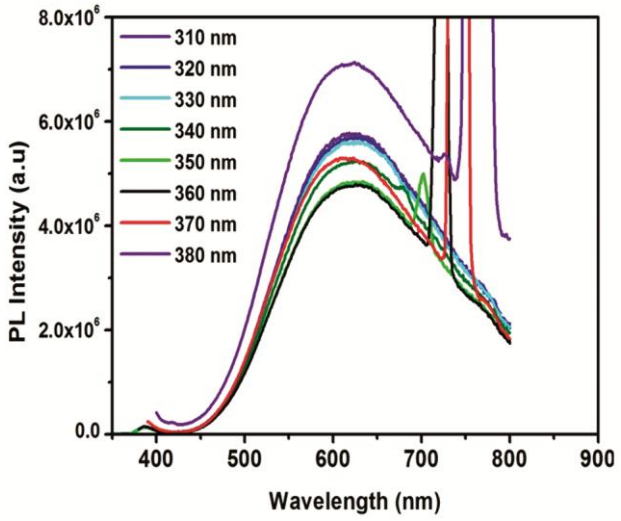

Fig. 7 — PL spectra of ZnO nanorods at different excitation wavelengths.

increased for excitation wavelengths 370 and 380 nm. The emission intensity decreased very significantly for excitation wavelengths above 380 nm. This result indicates that green and orange emissions can only be excited for excitation wavelengths above the conduction band edge.

As far as the initial and final states responsible for the orange emission are concerned, it is believed that the initial states are either conduction band or zinc interstitials and the final state is oxygen interstitial[2, 4, 10-11,14]. It was already revealed by many theoretical and experimental results that Zn_i is a shallow donor and the corresponding defect level will be located 0.22 eV below the conduction band edge[12,15]. However, there are other defects which can also introduce a level slightly below the conduction band edge and hydrogen defects is one such kind and it also introduces a defect level which is 0.05 eV below conduction band minimum[1]. From UV-v is and PLE results, it is clear that the defect levels for green and orange emissions are lies 0.04 and 0.1 eV below the conduction band. Moreover, formation of Zn_i defects requires high formation energy and hence there is a less possibility of formation of defect levels due to Zn_i below 0.05 eV[16]. However, the defects related to hydrogen and oxygen are easily formed in the hydrothermally grown ZnO nanorods and contribute to the visible emissions[1]. These results indicate that Zn_i defect level is not the initial state for green and orange emissions observed in this study. Hence, we believe that hydrogen related defects could be the initial levels which lie just below conduction band minimum.

On the other hand, oxygen interstitial defect has been considered as the final state responsible for the orange emission. As a matter of fact, oxygen interstitial defect introduces states in the lower part of the band gap that can accept two electrons. These states are derived from the oxygen p-orbital's and results in the deep acceptors which lies 0.79 or 1.59 eV above the valence band maximum[15,17]. In this study, the orange emission is observed at 620 nm (~ 2 eV) and the excitation wavelength dependent PL and PLE spectra shows the initial state responsible for the orange emission leis 0.1 eV below the conduction band. Hence the position of defect level (final state) responsible for the orange emission should be positioned 2.1 eV (2+0.1 eV) below the conduction band minimum. The band gap of ZnO nanorods in this study is 3.36 eV and oxygen interstitial level should be either 0.79 or 1.59 eV above the valance band maximum[12]. Moreover, the formation energy for the formation of oxygen interstitials is very high and hence there is less possibility for the formation of oxygen interstitial defects. On the other side, formation of hydrogen related defects in ZnO nanorods grown hydrothermally is certain. Hence the oxygen interstitial as a final level for the orange emission may be neglected. However, according to the PL and PLE results in this study, the defect level responsible for orange emission should be positioned at 2.1 eV below the conduction band minimum. It is well established that singly ionized oxygen vacancies forms a defect level which is 2 eV below the conduction band[15,18]. It is also reported that oxygen related defects increase in the nanorods of larger diameter[12] and we have observed maximum intensity for orange emission in larger diameter nanorods. Amin *et al*. in their recent study attributed emission at around 2 eV to the oxygen vacancies[8]. Hence, it may be concluded that the final state responsible for the orange emission could be defect level due to oxygen vacancies. Moreover, it can also be evident from these results that orange and green emissions can be effectively excited with excitation wavelengths above the band gap. Finally, based on our results it may be concluded that the initial and final states responsible for orange emission are defect levels due to hydrogen donors and oxygen vacancies respectively.

4 Conclusions

The structural and PL properties of ZnO nanorods of different aspect ratio were studied. ZnO nanorods showed strong and broad orange emission positioned

at 620 nm. It is observed that intensity of orange emission increased as the diameter of nanorods increase and larger diameter nanorods showed highest intensity. The initial and final states responsible for the orange emission are studied using UV-vis, PL, PLE and excitation wavelength dependent PL analysis of the samples. These results indicates that orange emission is due to the transition of an electron from a state which is positioned at around 0.05 eV below the conduction band to the defect level of singly ionized oxygen vacancies. Excitation wavelength dependent PL results showed that green emission and orange emissions can only be excited effectively at an excitation wavelengths near the conduction band edge and intensity decreased below and beyond the excitation energies.

References

1 Djurišić A, Leung Y, Tam K, Hsu Y, Ding L, Ge W, Zhong Y, Wong K, Chan W & Tam H, *Nanotechnology*, 18 (2007) 095702.

2 Jinpeng L & Meihua F, *Mater Lett*, 218 (2018) 18.

3 Angub M C M, Vergara C J T & Husay H A F, *J Lumin*, 203 (2018) 427.

4 Biroju R K & Giri P K, *J Appl Phys*, 122 (2017) 044302.

5 Chandrinou C, Boukos N, Stogios C & Travlos A, *J Microelectron*, 40 (2009) 296.

6 Gheisi A R, Neygandhi C, Sternig A K, Carrasco E, Marbach H, Thomelec D & Diwald O, *Phys Chem Chem Phys*, 16 (2014) 23922.

7 Sun W C, Yeh Y C, Ko C T, He J H & Chen M J, *Nanoscale Res Lett*, 6 (2011) 556.

8 Amine A, Mohammad I, Sorin V, Iftikhar A, Muhammad A A, Khalid S, Gheorghe D & Jean-Jacques P, *Nanomaterials*, 9 (2019) 794.

9 Greene L E, Law M, Goldberger J, Kim F, Johnson J C, Zhang Y F, Saykally R J & Yang P D, *Angew Chem Int Ed*, 42 (2003) 3031.

10 Zhang W C, Wu XL, Chen H T, Zhu J & Huang G S, *J Appl Phys*, 103 (2008) 093718.

11 Buryia M, Babina V, Changa Y Y, Remesa Z, Micovab J & Simek D, *Appl Surf Sci*, 525 (2020) 146448.

12 Zeng H, Duan G T, Li Y, Yang S K, Xu X X & Cai W P, *Adv Funct Mater*, 20 (2010) 561.

13 Yatskiv R & Grym J, *Superlattices Microstruct*, 99 (2016) 214.

14 Raji R & Gopchandran K G, *J Sci: Adv Mater Dev*, 2 (2017) 51.

15 Janotti A & Van de Walle C G, *Phys Rev B*, 76 (2007) 165202.

16 Sowri B K, Ramachandra R A & Venugopal R K, *J Lumin*, 158 (2015) 306.

17 Alvi N, Ul Hasan K, Nur O & Willander M, *Nanoscale Res Lett*, 6 (2011) 1.

18 Djuris˘ic´A B & Leung Y H, *Small*, 2 (2006) 944.